MODEL OF JOVIAN F REGION IONOSPHERE

(JOVIAN IONOSPHERE MODEL IN OFFSET DIPOLE APPROXIMATION)

by

A. TAN

PRINCIPAL INVESTIGATOR

SECOND ANNUAL REPORT OF NASA GRANT NAGW-1067

RESEARCH REPORT NO. AAMU-NAG-90-2

ALABAMA AGRICULTURAL AND MECHANICAL UNIVERSITY

NORMAL, ALABAMA 35762

OCTOBER 1990

CONTENTS

1. INTRODUCTION

The geomagnetic control of the earth's atmosphere is well understood. In the F-region and the topside ionosphere, non-electrical forces transport plasma along the magnetic field lines only. In consequence, the world-wide distribution of ionization is strongly dependent on the dip angle. For example, the equatorial anomaly is roughly symmetrical about the dipole equator rather than the geographic. The same appears to be the case in the Jovian ionosphere (Mahajan, 1981).

The influence of the magnetic field of Jupiter on its ionization pattern is one of several outstanding topics which need to be studied. Tan (1986) investigated the formation of equatorial anomaly in the Jovian ionosphere under a centered dipole model. Tan (1988) further studied the effect of the tilt of the Jovian dipole. The results were in broad agreement with those of a diffusive equilibrium model (Tan and Wu, 1981). In this study, an off-centered dipole model is constructed and its effects on the ionization pattern are investigated.

1.1. THE MAGNETIC FIELD OF JUPITER

Jupiter has the strongest magnetic field of any planet in the solar system. Its magnetic dipole, not unlike the earth's, is tilted approximately 10° from the rotational axis. In addition, significant quadrupole and octupole moments are present (Smith, et al., 1976; Acuna and Ness, 1976).

The Jovian magnetic field can be approximated as that due to an offset tilted dipole (OTD). A summary of the various OTD models can be found in Acuna, et al. (1983). The dipole is tilted approximately 10°

in the meridional plane of longitude 220° in System III (Fig. 1). The dipole is located at approximately 0.1 R_J in the equatorial plane at longitude 150°, R_J being the radius of Jupiter.

1.2. OBJECTIVE

A qualitative inspection would reveal the fact that the tilt effect of the dipole would be maximum in the meridional planes of longitudes 220° and 40° whereas the offset effect would be most prominent in the meridional planes of longitudes 150° and 330° (Tan and Wu, 1981; Tan, 1988). The latter effect is presently studied by a simple offset dipole model without tilt. The dipole is assumed to be situated in the meridional plane of longitude λ_{III} = 150°. Specifically, we study the differences in the ionization patterns in the meridional planes of λ_{III} = 150° (Western sector) and λ_{III} = 330° (Eastern sector) (see Dessler, 1983 for convention).

In the Jovian topside ionosphere, photoionization production rates and the loss rates are extremely slow. Hence significant diurnal variation is not expected and a diffusive equilibrium model is justified. In this model, it would be appropriate to take the electron density at the base as the observed peak electron density, which displays the existence of equatorial anomaly (Mahajan, 1981).

2. ECCENTRIC DIPOLE MODEL WITHOUT TILT

The Jovian magnetic field can be approximated as that of a dipole situated in the equatorial plane of Jupiter at a distance a = 0.1 R_J from the center (cf. Acuna, et al., 1983). In the present model, the tilt angle of the dipole from the rotational axis is neglected. Figure 2 depicts the meridional plane of longitude $\lambda_{III} = 150°$ which contains the dipole. The following systems of coordinates are defined in that plane:

(1) Planetocentric cartesian (x', z'),

(2) Planetocentric polar (r', θ'),

(3) Dipole castesian (x, z), and

(4) Dipole polar (r, θ) coordinates.

The transformation from (r, θ) to (r', θ') is effected in the following stages: (r, θ) -A→ (x, y) -B→ (x', z') -C→ (r', θ'), where the transformations A, B and C are given by

$$\text{A:} \quad x = r \sin\theta \ , \tag{2.1}$$

$$z = r \cos\theta \ , \tag{2.2}$$

$$\text{B:} \quad x' = x + a \ , \tag{2.3}$$

$$z' = z \ , \tag{2.4}$$

$$\text{C:} \quad r' = (x'^2 + z'^2)^{\frac{1}{2}} \ , \tag{2.5}$$

$$\theta' = \tan^{-1} \frac{x'}{z'} \ . \tag{2.6}$$

Substituting Eqs. (2.1) - (2.4) in (2.5) and (2.6), we get

$$r' = (r^2 + 2ar \sin\theta + a^2)^{\frac{1}{2}} \ , \tag{2.7}$$

and $\theta' = \tan^{-1}(\tan\theta + \frac{a}{r}\sec\theta)$. (2.8)

The inverse transformations from (r', θ') to (r, θ) are obtained by interchanging the primed and unprimed quantities and reversing the sign of a.

$$r = (r'^2 - 2ar' \sin\theta' + a^2)^{\frac{1}{2}} , \quad (2.9)$$

and $\theta = \tan^{-1}(\tan\theta' - \frac{a}{r'}\sec\theta')$. (2.10)

All equations (2.1) through (2.10) apply in the meridional plane of longitude $\lambda_{III} = 330°$ upon inversion of the sign of a.

2.1. DETERMINING THE COORDINATES OF THE FOOT OF THE FIELD LINE

For a dipole field line of definite L-value, the coordinates of the foot of the field line in the northern hemisphere $(r_o, \theta_o; r'_o, \theta'_o)$ can be calculated given the radial distance $r'_o = R_J + h_o = R$ (say), where h_o is the altitude of the base of the ionosphere. For a diffusive equilibrium model of the Jovian ionosphere, h_o is approximately the height of the maximum electron density (800 km), whereas R_J = 71,200 km, whence R = 72,000 km.

The foot of the field line is the point of intersection of the circle $r' = R$ and the dipole field line, whose equation is

$$r = L R_J \sin^2\theta . \quad (2.11)$$

Applying Eq. (2.11) in (2.7), we get

$$L^2 R_J^2 \sin^4\theta_o + 2aL R_J \sin^3\theta_o + a^2 - R^2 = 0. \quad (2.12)$$

One can solve for $y = \sin\theta_o$ numerically by the Newton-Raphson scheme (cf. Stark, 1970)

$$y'_{i+1} = y_i - \frac{f(y_i)}{f'(y_i)} \quad , \tag{2.13}$$

where $f(y_i) = L^2 R_J^2 \, y_i^4 + 2aLR_J \, y_i^3 + a^2 - R^2$, (2.14)

and $f'(y_i) = 4L^2 R_J^2 \, y_i^3 + 6aLR_J \, y_i^2$, (2.15)

whence $\theta_o = \sin^{-1} y$, (2.16)

$$r_o = LR_J \sin^2\theta_o \quad , \tag{2.17}$$

and $$\theta'_o = \tan^{-1}(\tan\theta_o + \frac{a}{r_o} \sec\theta_o) \quad . \tag{2.18}$$

The foot of the field line in the southern hemisphere then has the coordinates $(r_o, \theta_o + 90°; r'_o, \theta'_o + 90°)$.

2.2. DISTRIBUTION OF POINTS ALONG THE FIELD LINE

A couple of transformations introduced by Kendall (1962) and by Sterling, et al. (1969) have been found convenient in controlling the distribution of points along the field line:

$$q = -\frac{r_o^2 \cos\theta}{r^2} = \frac{\sin^4\theta_o \cos\theta}{\sin^4\theta} \quad , \tag{2.19}$$

and $$x = -\frac{\sinh(\Gamma q)}{\sinh(\Gamma q_o)} \quad . \tag{2.20}$$

Here q_o is the value of q at the foot of the field line in the northern hemisphere and Γ is an adjustable parameter which controls the distribution of points on the field line. A larger Γ for example distributes more points near the ends of the field line.

The arc length s is related to the dimensionless quantity x through

$$\frac{\partial}{\partial s} \equiv \gamma \frac{\partial}{\partial x} \quad , \tag{2.21}$$

$$\text{where} \quad \gamma = - \frac{(3\cos^2\theta + 1)^{\frac{1}{2}} \Gamma \cosh(\Gamma q)}{L^3 r_o \sin^6\theta \sinh(\Gamma q_o)} \quad . \tag{2.22}$$

2.3. LOCATING FIELD POINTS OVER THE LOCAL VERTICAL

In order to study the vertical profile of the ionosphere over a locality at a certain latitude, it is advantageous to choose points on field lines over the local vertical. The coordinates of the field point $(r', \theta'; r, \theta)$ are found from the intersection of the dipole field line with the line θ' = const. From Eqs. (2.10) and (2.11), we get

$$\tan\theta + \frac{a}{LR_J} \frac{(1 + u^2)^{3/2}}{u^2} - \tan\theta' = 0 \quad . \tag{2.23}$$

Letting $\tan\theta = u$, Eq. (2.23) can be written as

$$f(u) = u + \frac{a}{LR_J} \frac{(1 + u^2)^{3/2}}{u^2} - \tan\theta' = 0 \quad . \tag{2.24}$$

$$\text{Then} \quad f'(u) = 1 + \frac{a}{LR_J} \left[\frac{3(1 + u^2)^{3/2}}{u} - \frac{2(1 + u^2)^{3/2}}{u^3} \right] \quad , \tag{2.25}$$

and the Newton-Raphson scheme for $u = \tan\theta$ is given by

$$u_{i+1} = u_i - \frac{f(u_i)}{f'(u_i)} \quad . \tag{2.26}$$

Thus, given θ', the coordinates of the field point can be calculated.

$$\theta = \tan^{-1} u \quad , \tag{2.27}$$

$$r = LR_J \sin^2\theta \quad , \tag{2.28}$$

and $$r' = (r^2 + 2ar \sin\theta + a^2)^{\frac{1}{2}} \quad . \tag{2.29}$$

2.4. COMPONENT OF GRAVITY ALONG FIELD LINE

The component of the gravitational acceleration g along the field line is given by (vide Fig.3)

$$g_s = - g \sin I' \quad , \tag{2.30}$$

where I' is the true dip angle. If I is the dip angle in the centered dipole model, then

$$I' = I + \theta' - \theta \quad . \tag{2.31}$$

Now, $$\tan I = 2 \cot\theta \quad . \tag{2.32}$$

Substituting from Eqs. (2.32) and (2.8) in (2.31) and simplifying, we get

$$I' = \tan^{-1} \frac{2(\tan\theta + \cot\theta) - \frac{3a}{r} \sec\theta}{\sec^2\theta - \frac{a}{r} \sec\theta \, (\tan\theta - 2 \cot\theta)} \quad . \tag{2.33}$$

Taking into account the radial dependence of g, we have

$$g_s = g_o \frac{R^2}{r'^2} \sin I' \quad , \tag{2.34}$$

where g_o is the acceleration of gravity at the foot of the field line,

and r' and I' are given by Eqs. (2.7) and (2.33) respectively.

In terms of a sole coordinate θ,

$$r'^2 = L^2 R_J^2 \sin^4\theta + 2aLR_J \sin^3\theta + a^2 \quad , \tag{2.35}$$

and $$I' = \tan^{-1} \frac{2\,(\tan\theta + \cot\theta) - \frac{3a}{LR_J} \sec\theta \operatorname{cosec}^2\theta}{\sec^2\theta - \frac{a}{LR_J} \sec\theta \operatorname{cosec}^2\theta\,(\tan\theta - 2\cot\theta)} \quad . \tag{2.36}$$

2.5. COMPONENT OF CENTRIFUGAL ACCELERATION ALONG FIELD LINE

The component of the centrifugal acceleration along the dipole field line is (vide Fig.3)

$$f_s = \Omega^2 r' \sin\theta' \cos(I' - \theta') \quad . \tag{2.37}$$

Since $I' - \theta' = I - \theta$, we have (from Tan, 1979)

$$\cos(I' - \theta') = \frac{3 \cos\theta \sin\theta}{(3\cos^2\theta + 1)^{\frac{1}{2}}} \quad . \tag{2.38}$$

Further, from Fig. 2, we have

$$r' \sin\theta' = r \sin\theta + a \quad , \tag{2.39}$$

whence

$$f_s = \frac{3\,\Omega^2 (r \sin\theta + a) \sin\theta \cos\theta}{(3\cos^2\theta + 1)^{\frac{1}{2}}} \quad . \tag{2.40}$$

In terms of θ only, Eq. (2.40) can be written as

$$f_s = \frac{3\,\Omega^2 (LR_J \sin^3\theta + a) \sin\theta \cos\theta}{(3\cos^2\theta + 1)^{\frac{1}{2}}} \quad . \tag{2.41}$$

3. THEORY

The predominant ion in the Jovian ionosphere is proton (H^+). In the absence of electromagnetic drift, the governing equation of the ions along the magnetic field lines is given by (cf. Tan, 1986)

$$\frac{\partial N}{\partial t} + \frac{\partial}{\partial s}(NV_s) + BNV_s \frac{\partial}{\partial s}(\frac{1}{B}) = \alpha - \beta N \quad , \tag{3.1}$$

where N = number density of ions/electrons,

V_s = velocity of ions along magnetic field lines,

B = magnetic field intensity,

s = arc length along B,

t = local time,

α = production rate of ions,

and β = loss coefficient of ions.

Now the topside ionospheric plasma can be approximated by a diffusive equilibrium distribution (cf. Bauer, 1969). This is even more true for the Jovian ionosphere, since the loss rate for protons is very slow. Under diffusive equilibrium conditions, Eq. (3.1) reduces to an ordinary differential equation

$$\frac{d}{ds}(NV_s) + BNV_s \frac{d}{ds}(\frac{1}{B}) = 0 \quad . \tag{3.2}$$

In the Jovian ionosphere, the electrons, ions and neutrals are assumed to be in thermal equilibrium (Henry and McElroy, 1969; Nagy, et al., 1976). The velocity V_s is then given by (cf. Tan, 1986)

$$V_s = \frac{1}{m\nu}[mg_s + mf_s - \frac{2}{N}\frac{d}{ds}(NkT)] \quad , \tag{3.3}$$

where m = proton mass,

ν = ion-neutral collision frequency,

k = Boltzmann's constant,

and T = temperature.

By substituting Eq. (3.3) into Eq. (3.2), we have

$$P' \frac{d^2N}{ds^2} + Q' \frac{dN}{ds} + R'N = 0 \quad , \tag{3.4}$$

with $$P' = \frac{2kT}{m\nu} \quad , \tag{3.5}$$

$$Q' = \frac{2k}{m} \left[\frac{1}{\nu} \frac{dT}{ds} + \frac{d}{ds} \left(\frac{T}{\nu}\right) + \frac{T}{\nu} B \frac{d}{ds} \left(\frac{1}{B}\right)\right] - \frac{g_s+f_s}{\nu} \quad , \tag{3.6}$$

and $$R' = \frac{2k}{m} \left[\frac{d}{ds}\left(\frac{1}{\nu} \frac{dT}{ds}\right) + \frac{1}{\nu} \frac{dT}{ds} B \frac{d}{ds}\left(\frac{1}{B}\right)\right] - \frac{d}{ds}\left(\frac{g_s+f_s}{\nu} \right) - \frac{g_s+f_s}{\nu} B \frac{d}{ds}\left(\frac{1}{B}\right) \tag{3.7}$$

Applying the transformation from s to x via Eq. (2.21), we get

$$P \frac{d^2N}{dx^2} + Q \frac{dN}{dx} + RN = 0 \quad , \tag{3.8}$$

with $$P = \gamma^2 P' \quad , \tag{3.9}$$

$$Q = \gamma P' \frac{d\gamma}{dx} + Q' \quad , \tag{3.10}$$

and $$R = R' \quad . \tag{3.11}$$

Equation (3.8) can be rewritten as

$$\frac{d^2N}{dx^2} + a \frac{dN}{dx} + bN = 0 \quad , \tag{3.12}$$

where $a = \frac{Q}{P}$, (3.13)

and $b = \frac{R}{P}$. (3.14)

Equation (3.12) can now be solved by a standard numerical procedure. Rewriting N as y and dN/dx as z, we have two simultaneous first order differential equations

$$\frac{dy}{dx} = z = f_1(x, y, z) \quad , \tag{3.15}$$

and $$\frac{dz}{dx} = -az - by = f_2(x, y, z) \quad . \tag{3.16}$$

Equations (3.15) and (3.16) can be solved by the Runge-Kutta scheme applied separately (cf. Stark, 1970)

$$y_{i+1} = y_i + \frac{1}{6}(k_1 + 2k_2 + 2k_3 + k_4) \quad , \tag{3.17}$$

$$z_{i+1} = z_i + \frac{1}{6}(c_1 + 2c_2 + 2c_3 + c_4) \quad , \tag{3.18}$$

where $$k_1 = f_1(x_i, y_i, z_i)w \quad , \tag{3.19}$$

$$c_1 = f_2(x_i, y_i, z_i)w \quad , \tag{3.20}$$

$$k_2 = f_1(x_i + \frac{w}{2}, y_i + \frac{k_1}{2}, z_i + \frac{c_1}{2})w \quad , \tag{3.21}$$

$$c_2 = f_2(x_i + \frac{w}{2}, y_i + \frac{k_1}{2}, z_i + \frac{c_1}{2})w \quad , \tag{3.22}$$

$$k_3 = f_1(x_i + \frac{w}{2}, y_i + \frac{k_2}{2}, z_i + \frac{c_2}{2})w \quad , \tag{3.23}$$

$$c_3 = f_2(x_i + \frac{w}{2}, y_i + \frac{k_2}{2}, z_i + \frac{c_2}{2})w \quad , \tag{3.24}$$

$$k_4 = f_1(x_i + w,\ y_i + k_3,\ z_i + c_3)w \quad , \tag{3.25}$$

and $$c_4 = f_2(x_i + w,\ y_i + k_3,\ z_i + c_3)w \quad . \tag{3.26}$$

In Eqs. (3.19) through (3.26), w is the step size, i.e., Δx.

3.1. STATIC DIFFUSIVE EQUILIBRIUM

The condition of static diffusive equilibrium, which is applicable to the topside ionosphere, is given by $V_s = 0$ (cf. Bauer, 1969). Then Eq. (3.3) can be integrated, by separation of variables, to give

$$N = \frac{N_o T_o}{T}\, e^{\int_o^s \frac{m}{2kT}(g_s + f_s)\, ds} \quad . \tag{3.27}$$

The differential arc length in terms of θ is

$$ds = LR_J\,(3\cos^2\theta + 1)^{\frac{1}{2}} \sin\theta\, d\theta \quad . \tag{3.28}$$

Equation (3.28) can be integrated from the foot of the field line in the northern hemisphere (cf. Chapman and Sugiura, 1956) to give

$$s = LR_J\,[\cos\theta_o(3\cos^2\theta_o + 1)^{\frac{1}{2}} - \cos\theta\,(3\cos^2\theta + 1)^{\frac{1}{2}}]$$

$$+ \frac{LR_J}{\sqrt{3}} \ln \frac{\sqrt{3}\cos\theta_o + (3\cos^2\theta_o + 1)^{\frac{1}{2}}}{\sqrt{3}\cos\theta + (3\cos^2\theta + 1)^{\frac{1}{2}}} \quad . \tag{3.29}$$

In terms of the variable x (whose values range from -1 at the foot of the field line in the northern hemisphere through naught at the dipole equator to +1 at the foot of the field line in the southern hemisphere), Eq. (3.27) assumes the form

$$N = \frac{N_o T_o}{T} e^{\int_{-1}^{x} \frac{m}{2kT} (g_s + f_s) \frac{dx}{\gamma}} , \qquad (3.30)$$

where γ is given by Eq. (2.22).

3.2. INPUT DATA

In the diffusive equilibrium model, it is appropriate to take the electron density at the base as the peak electron density. The observed peak electron density in the Jovian ionosphere, displaying equatorial anomaly, has been fitted with the expression (Tan, 1986)

$$N_o = 0.18 + 0.0367 \lambda^{3/2} - 0.004056 \lambda^2 , \qquad (3.31)$$

where λ is the absolute value of the latitude in degrees and N_o is expressed in 10^5 electrons/cm^3. Figure 4 shows the latitudinal variation of N_o as given by the expression (3.30).

The altitude of the base is taken as the height of the observed peak electron density, which is approximately equal to 800 km (see, for example, Mahajan, 1987).

The altitudinal variation of the temperature is taken from Atreya, et al. (1981) and Festou, et al. (1981). The temperature is assumed to increase linearly from 600°K at 800 km to 1200°K at 1400 km. The temperature above 1400 km is assumed to have the constant value of 1200°K.

4. RESULTS AND DISCUSSIONS

Figures 5 through 9 illustrate the results of our calculations. In Fig. 5, contour plots of the electron density in the longitudinal planes of both Western and Eastern Sectors are shown together with the dipole field lines. In general, the electron densities are higher in the Western Sector than in the Eastern. This is a direct consequence of the configuration of the dipole field lines in the two Sectors. In the Western Sector, the ions can diffuse along the field lines to higher altitudes from the base at the same latitude, thereby producing greater electron densities in the plasmasphere.

Also shown in Fig. 5 are the loci of points at which the components of gravitational and centrifugal forces along the field lines are equal and opposite. In the region of centrifugal dominance, the electron density slowly increases with distance, thus creating a region of enhanced electron density away from the planet. As a result, the troughs of electron densities are found at midlatitude heights (λ = 20° to 30° in the Western Sector and λ = 20° to 25° in the Eastern Sector) rather than above the equator. Above the equator, the electron density profile possesses a minimum which is the saddle point in the electron density contour.

Figures 6 and 7 show the vartical profiles of electron density in the two Sectors above the equator (latitude λ= 0°) and a midlatitude location (λ = 30°). As stated earlier, the latitudinal variation of the electron density at the base was given Eq. (3.31) to reflect the observed electron density. The electron densities were generally lower above the equator than at the midlatitude location owing to the boundary

conditions used. However, this situation is reversed above 6500 km in the Western Sector and above 9500 km in the Eastern. This means that the equatorial anomaly does not translate into the plasmaspheric heights. As stated above, the electron densities are always greater in the Western Sector compared with those in the Eastern.

The plasma scale heights were also greater above the equator and in the Western Sector. The difference in the scale heights between the two Sectors above the equator (1700 km vs. 1360 km) was particularly significant. This difference ought to betray itself if enough observational data were available. The calculated scale heights were generally larger than those observed which ranged from 540 km to 1040 km (cf. Mahajan, 1987).

Figures 8 and 9 show the vertical profiles of electron density in the plasmasphere above the equator and the midlatitude location respectively. The gradients of the curves become steeper with altitude and consequently the scale height becomes larger. This is due to the fact that the centrifugal force on the corotating plasma increases with the radial distance as the gravitational force decreases.

As the electron density curve becomes steeper with altitude, the electron density may undergo a minimum and actually increase with altitude thereafter. Figure 10, which is an extension of Fig. 8 to include higher altitudes actually shows this. This would be true so long as the assumption of the corotation of plasma is valid. As for the limits of corotation on Jupiter, the reader is referred to an article by Hill (1979).

4.1. FURTHER STUDY

This simplified model has been conveniently applied to study the ionization patterns in the meridional planes of maximum offset effect. The ionization patterns in the other meridional planes would be intermediate between the two extreme cases studied. However, in the other sectors, the mathematical expressions would be much more complicated. Further studies on the effect of the planetary magnetic field on the ionosphere would include the following topics.

(1) Saturnian ionosphere model in the offset dipole approximation. The magnetic field of Saturn is more purely dipolar than Jupiter's with the dipole axis within 1° of the rotational axis. The dipole is off-centered by about 0.04 R_S to the north. Here the longitudinal differences in the ionization patterns would not be significant. But the offset effect would produce differences between the ionizations in the northern and southern hemispheres. A simplified model along the lines of this study can be easily constructed.

(2) Offset dipole model with tilt. The most general dipole model is that of an offset and tilted dipole. For Jupiter, the dipole could be taken as lying in the equatorial plane. This assumption fetched a great deal simplification in the mathematical expressions. However, in the case of Uranus or Neptune, this luxury cannot be afforded. The magnetic dipoles of both these outer planets are highly eccentric and tilted. Here one needs a general offset and tilted dipole model to study the magnetic field effect on the ionization patterns. Needless to say, this will be a much formidable challenge for the modeller.

REFERENCES

M. H. Acuna and N. F. Ness in Jupiter, T. Gehrels ed., University of Arizona Press, 1976.

M. H. Acuna, K. W. Behannon and J. E. P. Connerney in Physics of the Jovian magnetosphere, A. J. Dessler, ed., Cambridge University Press, 1983.

S. K. Atreya, T. M. Donahue and M. C. Festou, Astrophys. J. Lett., 247, L43, 1981.

S. J. Bauer, Proc. IEEE, 57, 1114, 1969.

S. Chapman and M. Sugiura, J. Geophys. Res., 61, 485, 1956.

A. J. Dessler in Physics of the Jovian magnetosphere, A. J. Dessler ed., Cambridhe University Press, 1983.

M. C. Festou, S. K. Atreya, T. M. Donahue, B. R. Sandel, D. E. Schemansky and A. L. Broadfoot, J. Geophys. Res., 86, 5715, 1981.

R. J. W. Henry and M. B. McElroy, J. Atmos. Sci., 26, 912, 1969.

T. W. Hill, J. Geophys. Res., 84, 6554, 1979.

P. C. Kendall, J. Atmos. Terr. Phys., 24, 805, 1962.

K. K. Mahajan, Geophys. Res. Lett., 8, 66, 1981.

K. K. Mahajan, Ind. J. Rad. Space Phys., 16, 192, 1987.

A. F. Nagy, W. L. Chameides, R. H. Chan and S. K. Atreya, J. Geophys. Res., 81, 5567, 1976.

E. J. Smith, L. Davis, Jr. and D. E. Smith in Jupiter, T. Gehrels ed., University of Arizona Press, 1976.

D. L. Sterling, W. B. Hanson, R. J. Moffett and R. G. Baxter, Radio Sci., 4, 1005, 1969.

P. A. Stark, Introduction to Numerical Methods, The MacMillan Co., New York, 1970.

A. Tan, Ph. D. Dissertation, University of Alabama in Huntsville, 1979.

A. Tan, Planet. Space Sci., 34, 117, 1986.

A. Tan, Final Project Report of NSF Grant ATN-8611625, Alabama A&M University, 1988.

A. Tan and S. T. Wu, Geofis. Intl., 20, 11, 1981.

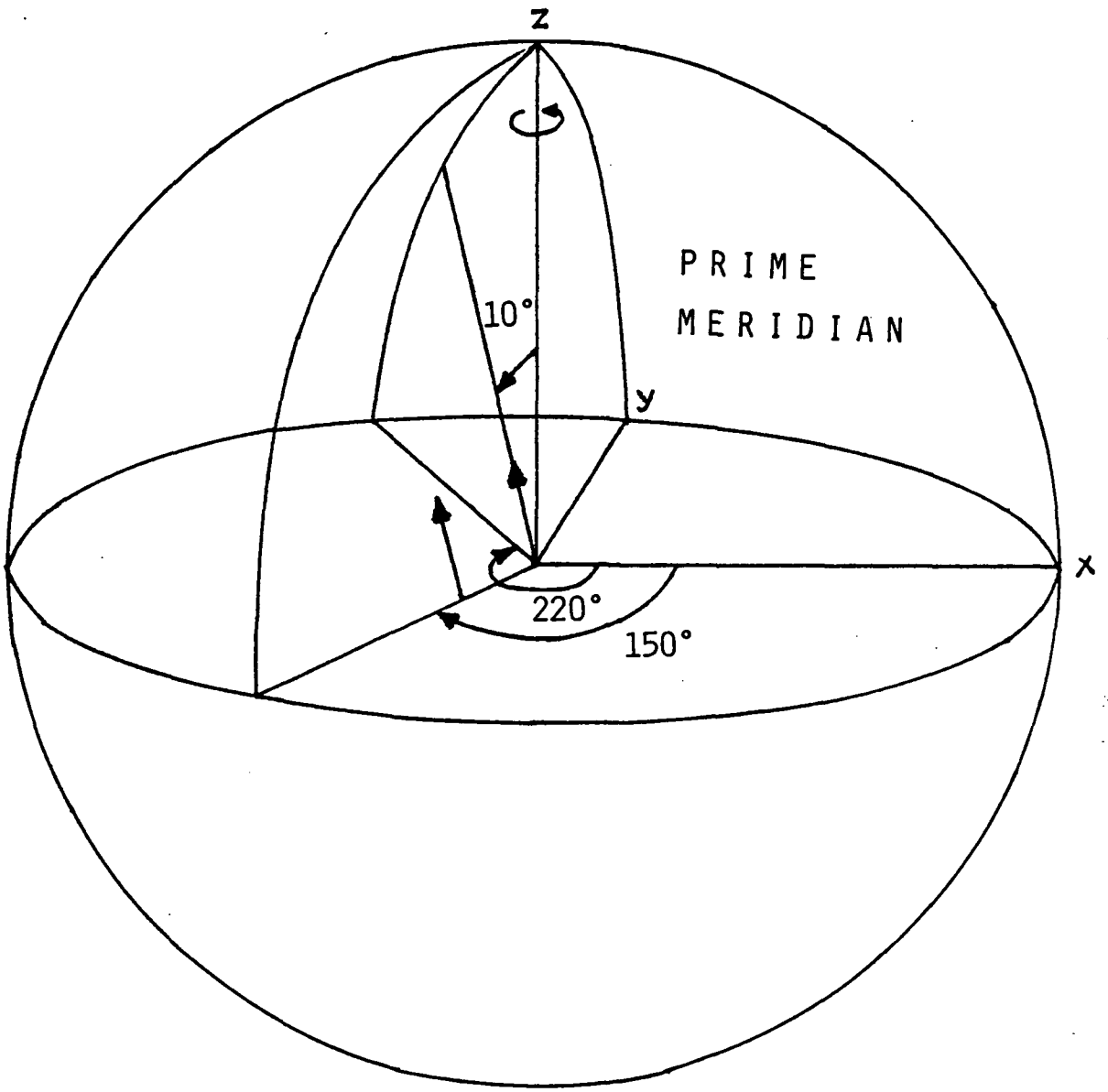

Fig.1. The Jovian dipole in System III. The dipole is tilted 10° in the meridional plane of longitude 220°. The dipole is located at 0.1 R_J in the equatorial plane of Jupiter at longitude 150°.

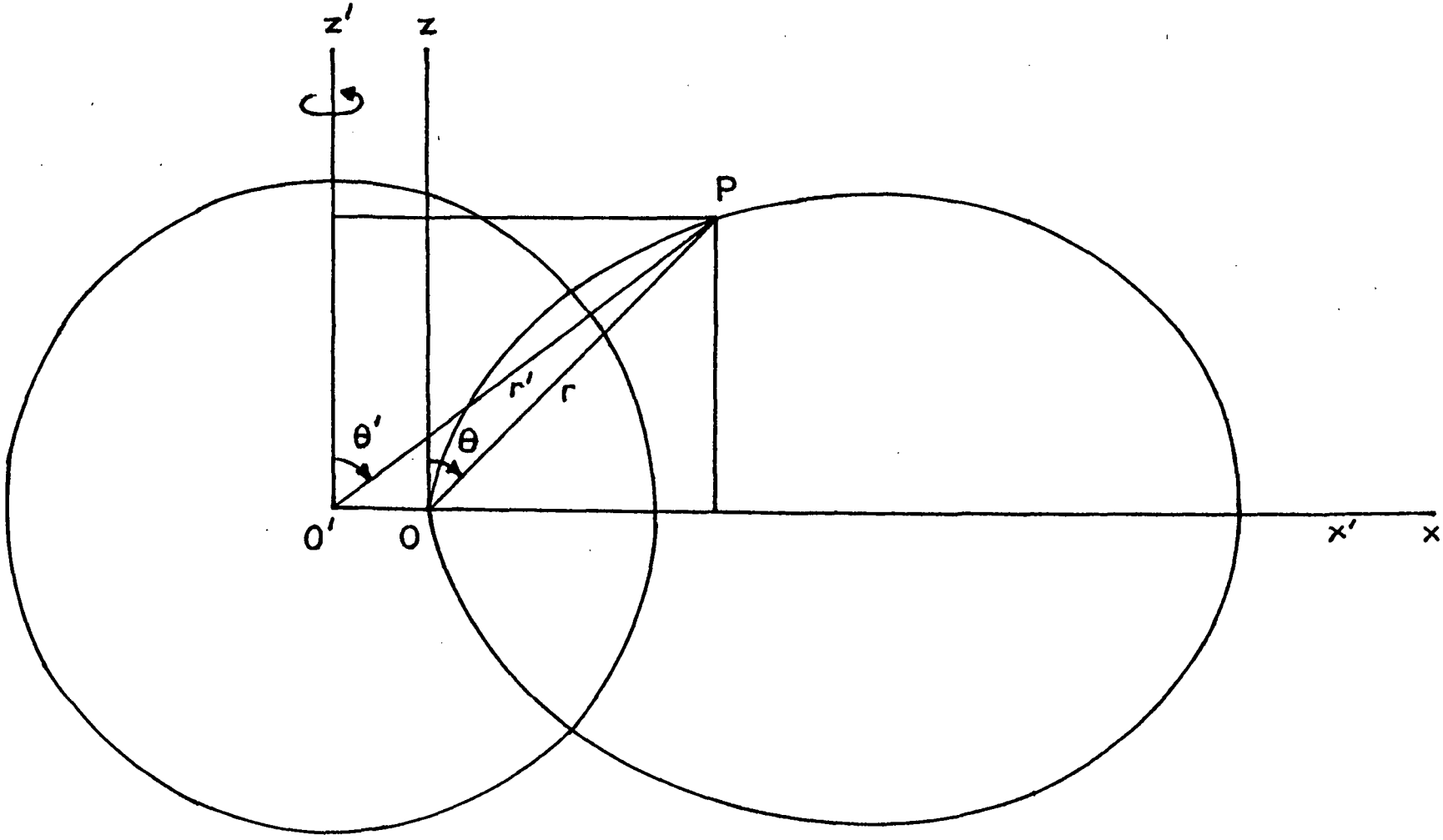

Fig.2. Planetocentric Cartesian (x',z'), Planetocentric Polar (r', θ'), Dipole Cartesian (x, z) and Dipole Polar (r, θ) Coordinates.

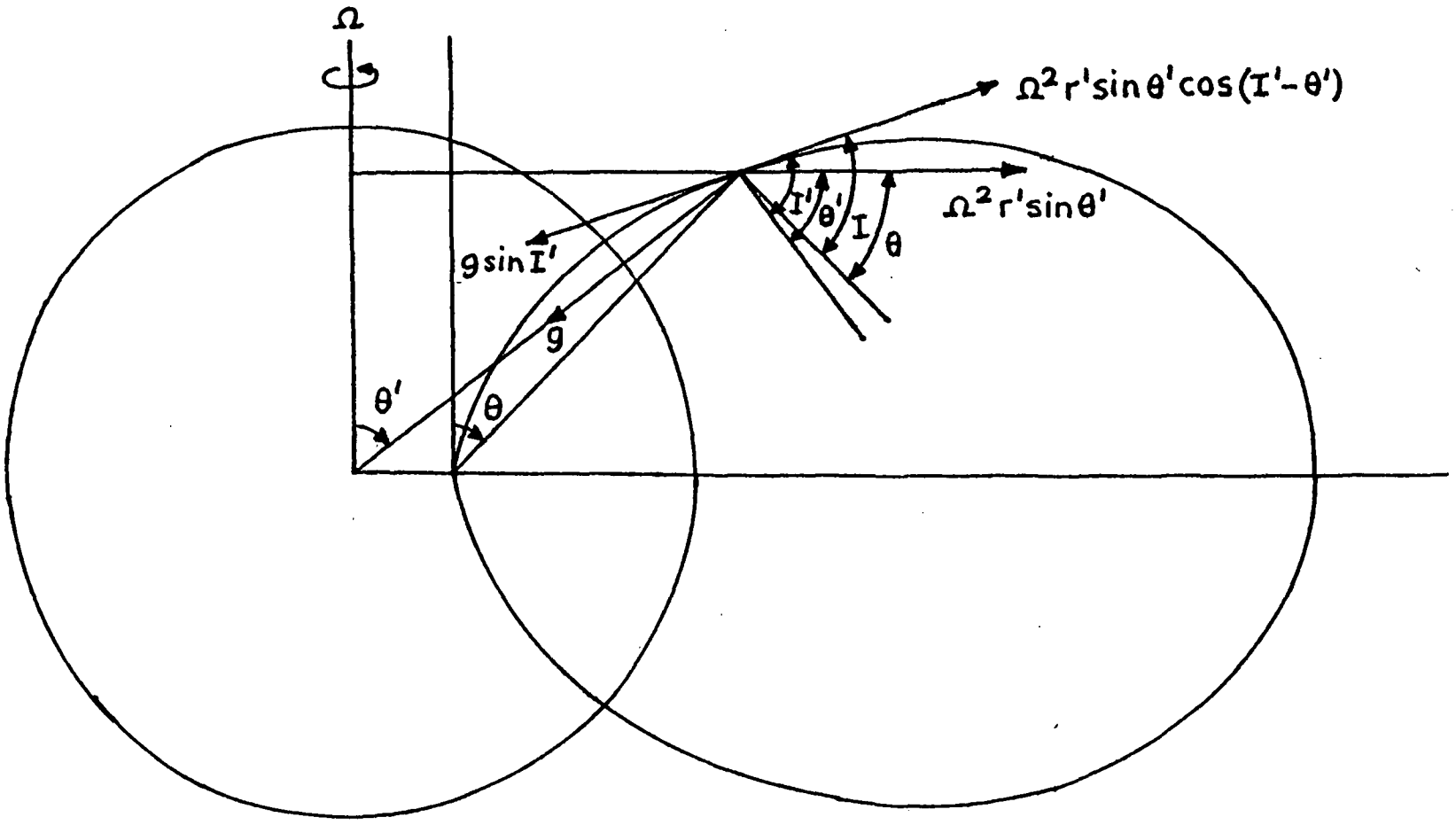

Fig.3. Components of gravity and centrifugal force along dipole field line.

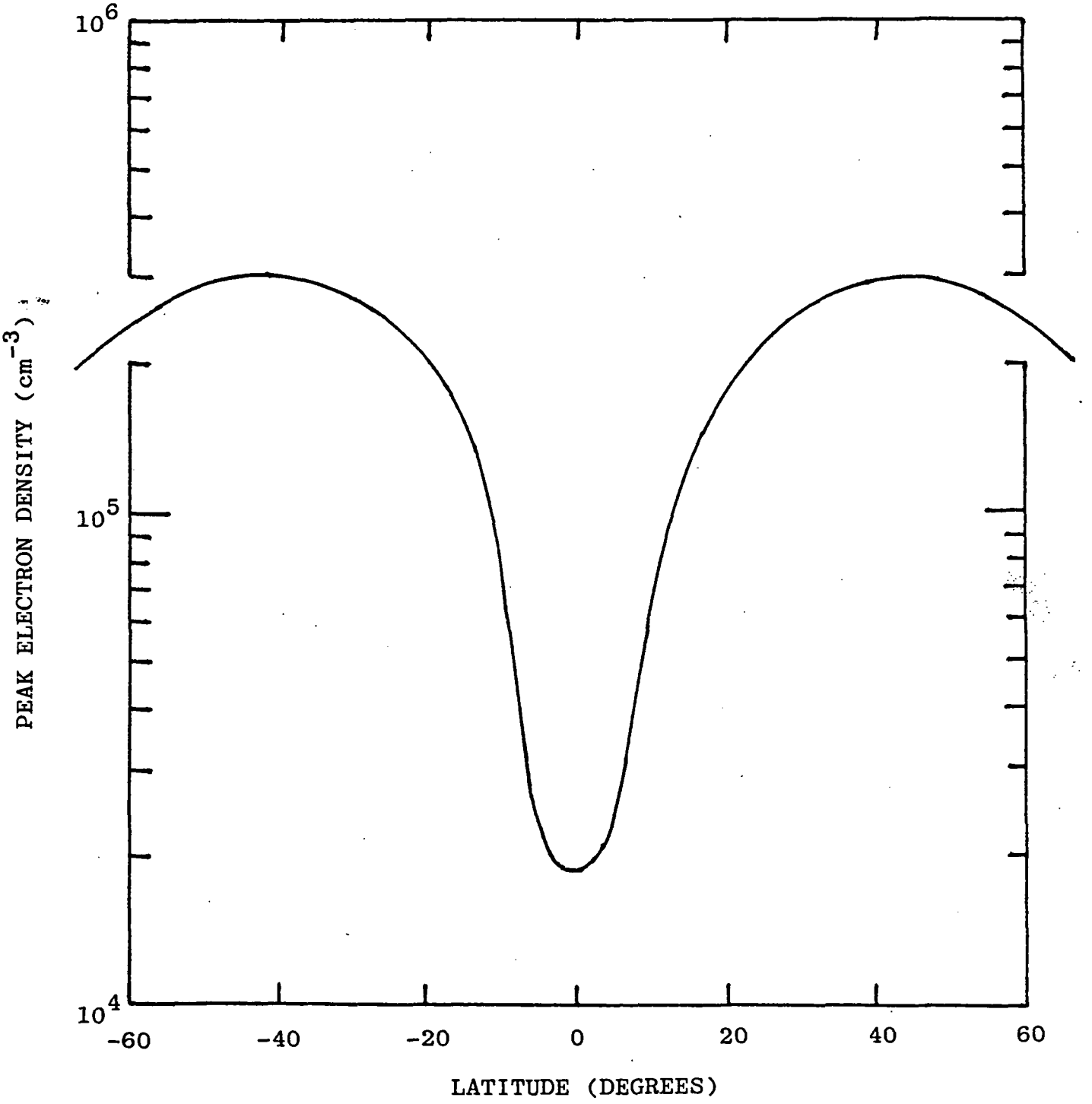

Fig.4. Least-square fit of observed latitudinal variation of peak electron density.

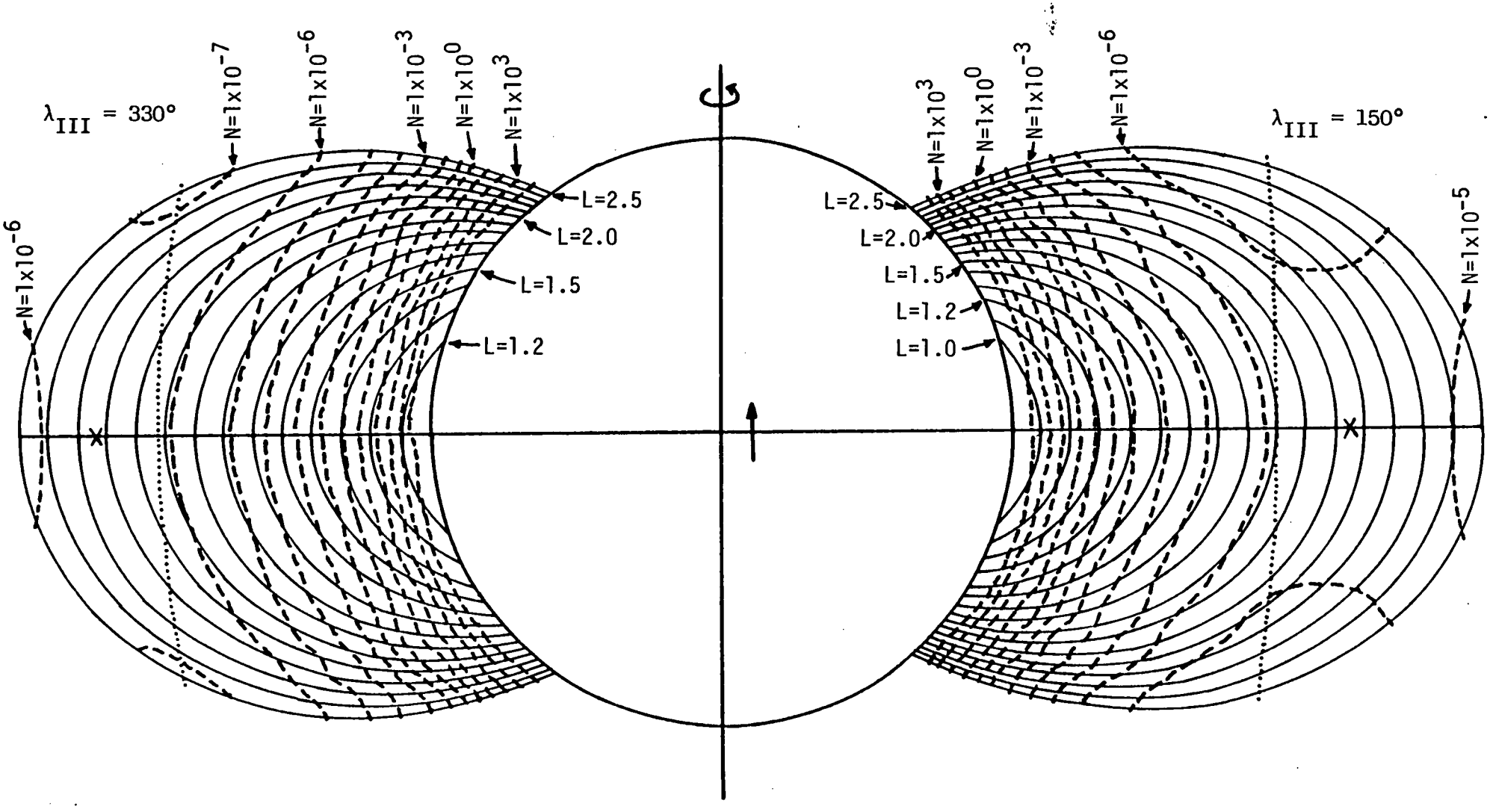

Fig.5. Contour plot of electron density in the meridional planes of longitudes 150° (Western Sector) and 330° (Eastern Sector) in the eccentric dipole model. The solid lines are dipole field lines whereas the dashed lines are contours of constant electron density. The dotted lines are loci of points at which the components of gravity and centrifugal forces along the filed lines are equal and opposite. The cross marks are the saddle points in the electron density contours.

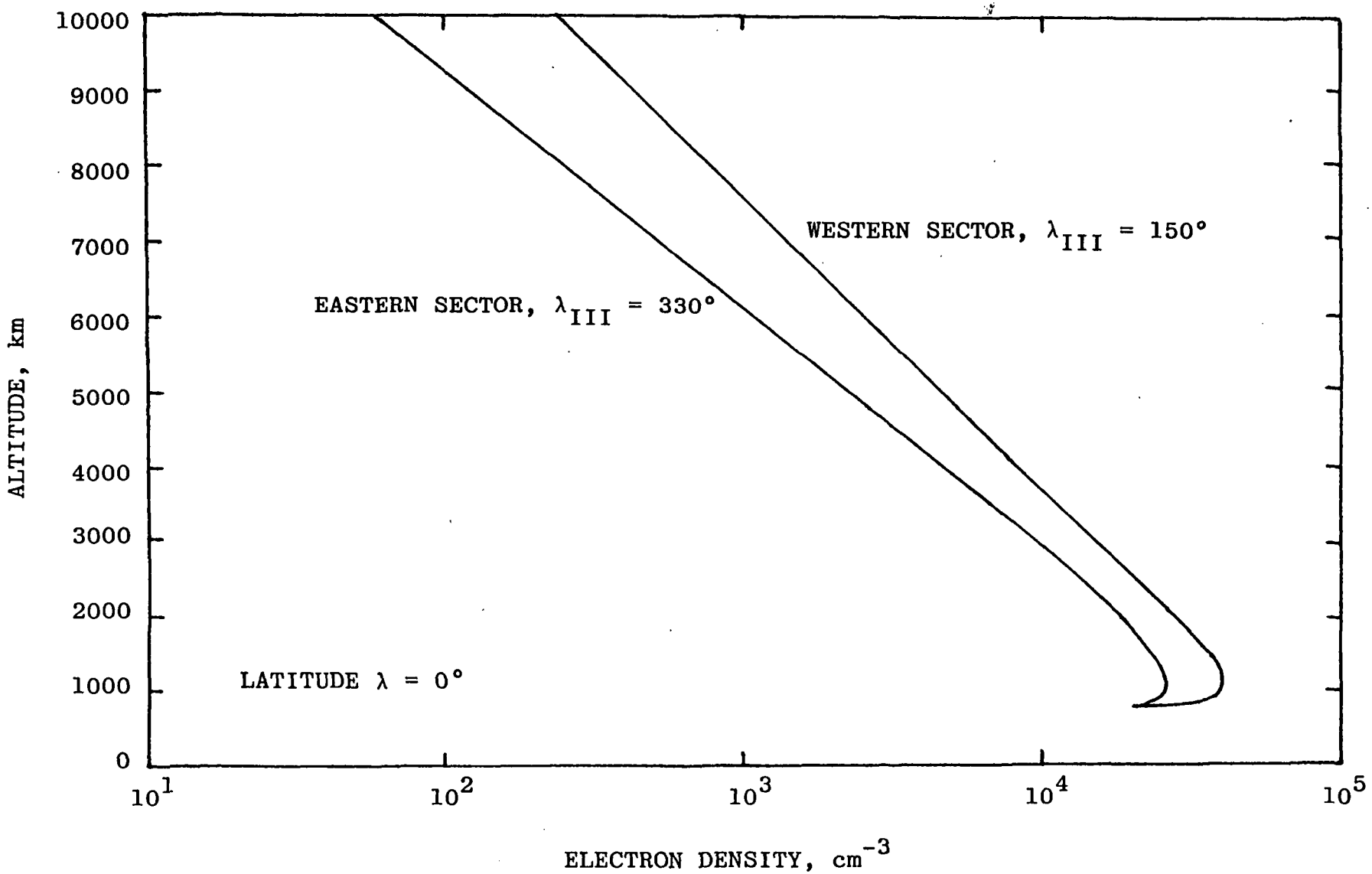

Fig.6. Vertical profiles of electron density in the topside equatorial ionospheres ($\lambda = 0°$) in the Western ($\lambda_{III} = 150°$) and Eastern ($\lambda_{III} = 330°$) Sectors. The plasma scale heights are 1700 km and 1360 km in the Western and Eastern Sectors respectively.

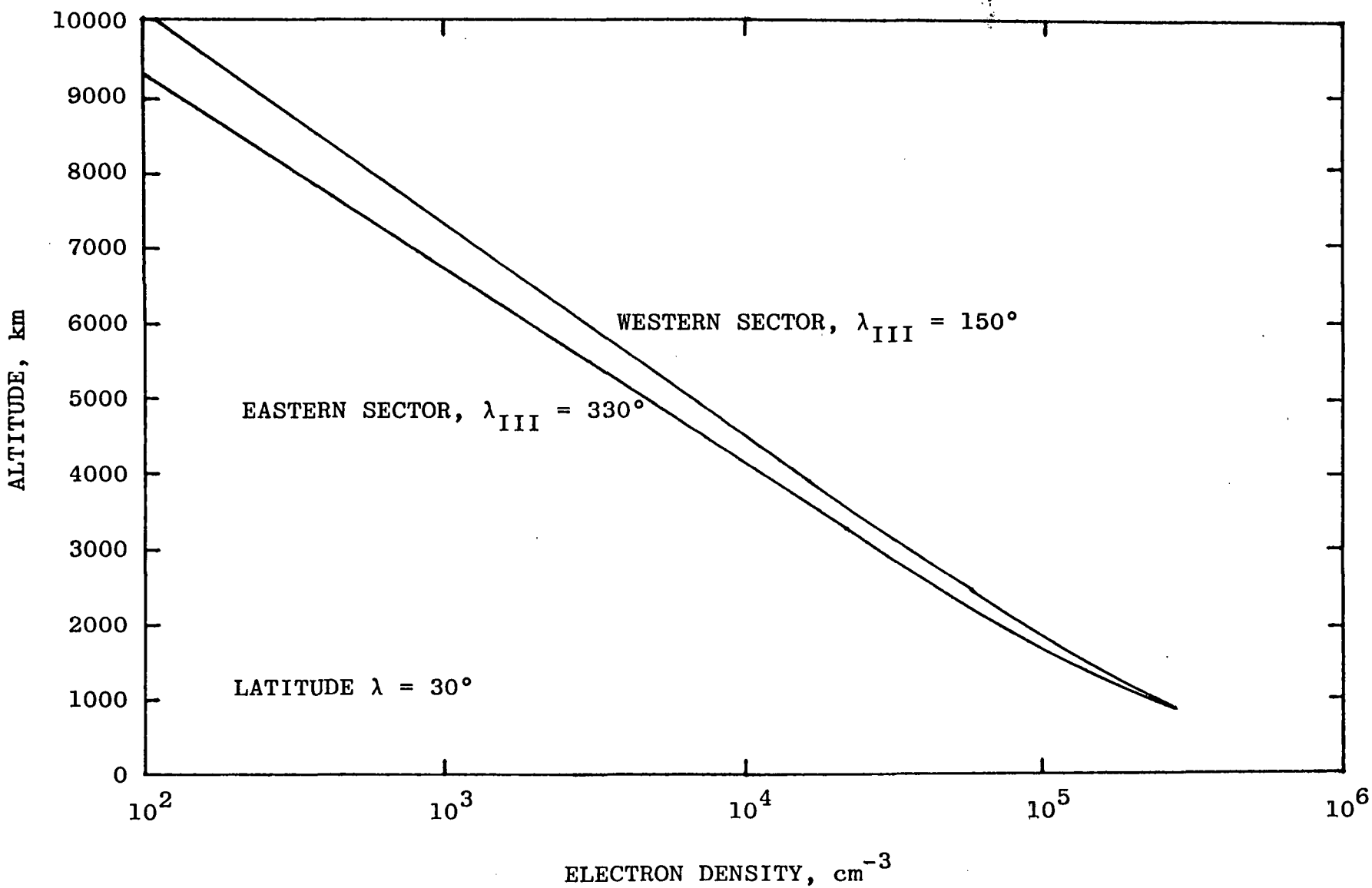

Fig.7. Vertical profiles of electron density in the topside ionospheres at latitude $\lambda = 30°$ in the Western ($\lambda_{III} = 150°$) and Eastern ($\lambda_{III} = 330°$) Sectors. The plasma scale heights are 1200 km and 1110 km in the Western and Eastern Sectors respectively.

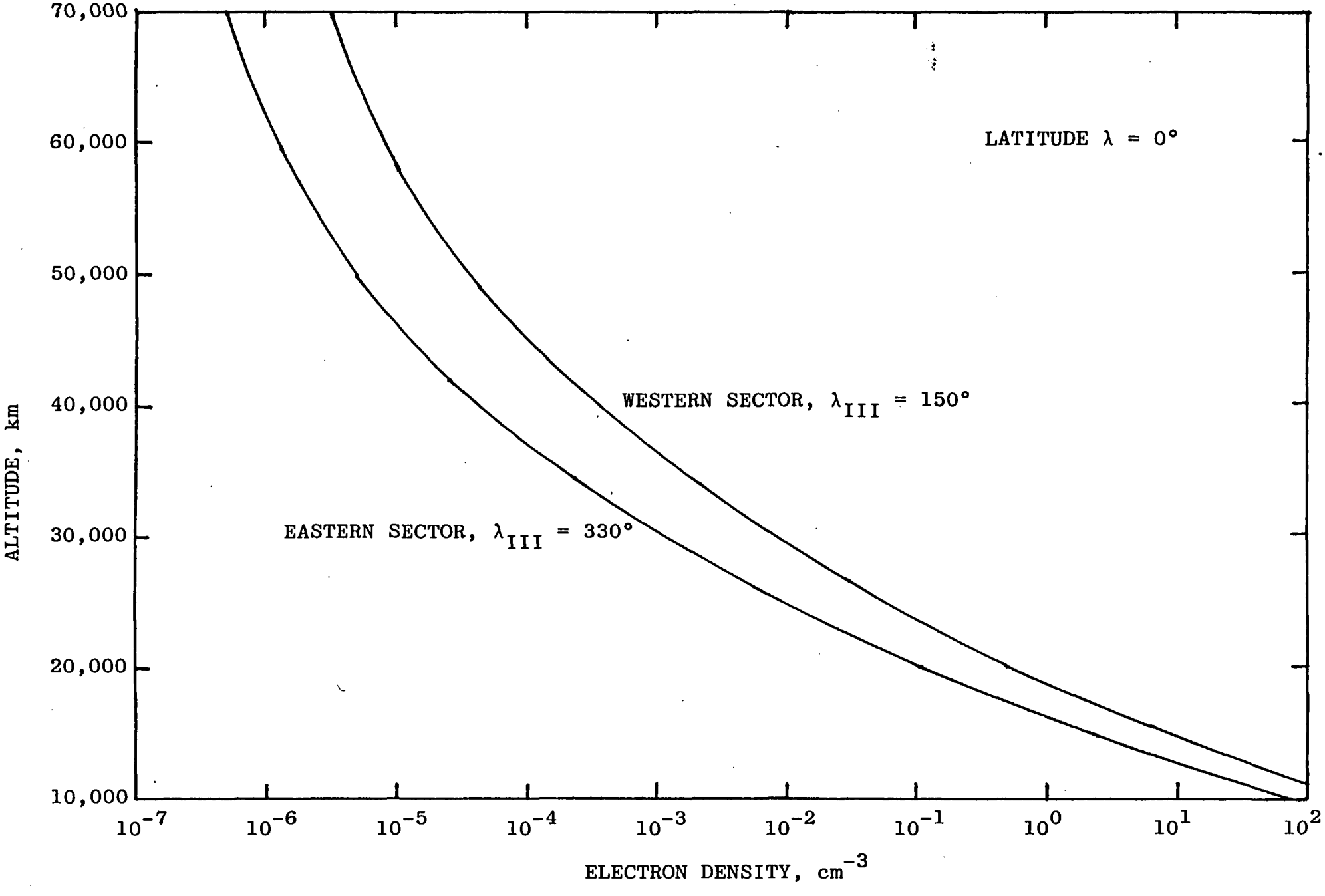

Fig.8. Vertical profiles of electron density in the equatorial plasmaspheres ($\lambda = 0°$) in the Western ($\lambda_{III} = 150°$) and Eastern ($\lambda_{III} = 330°$) Sectors.

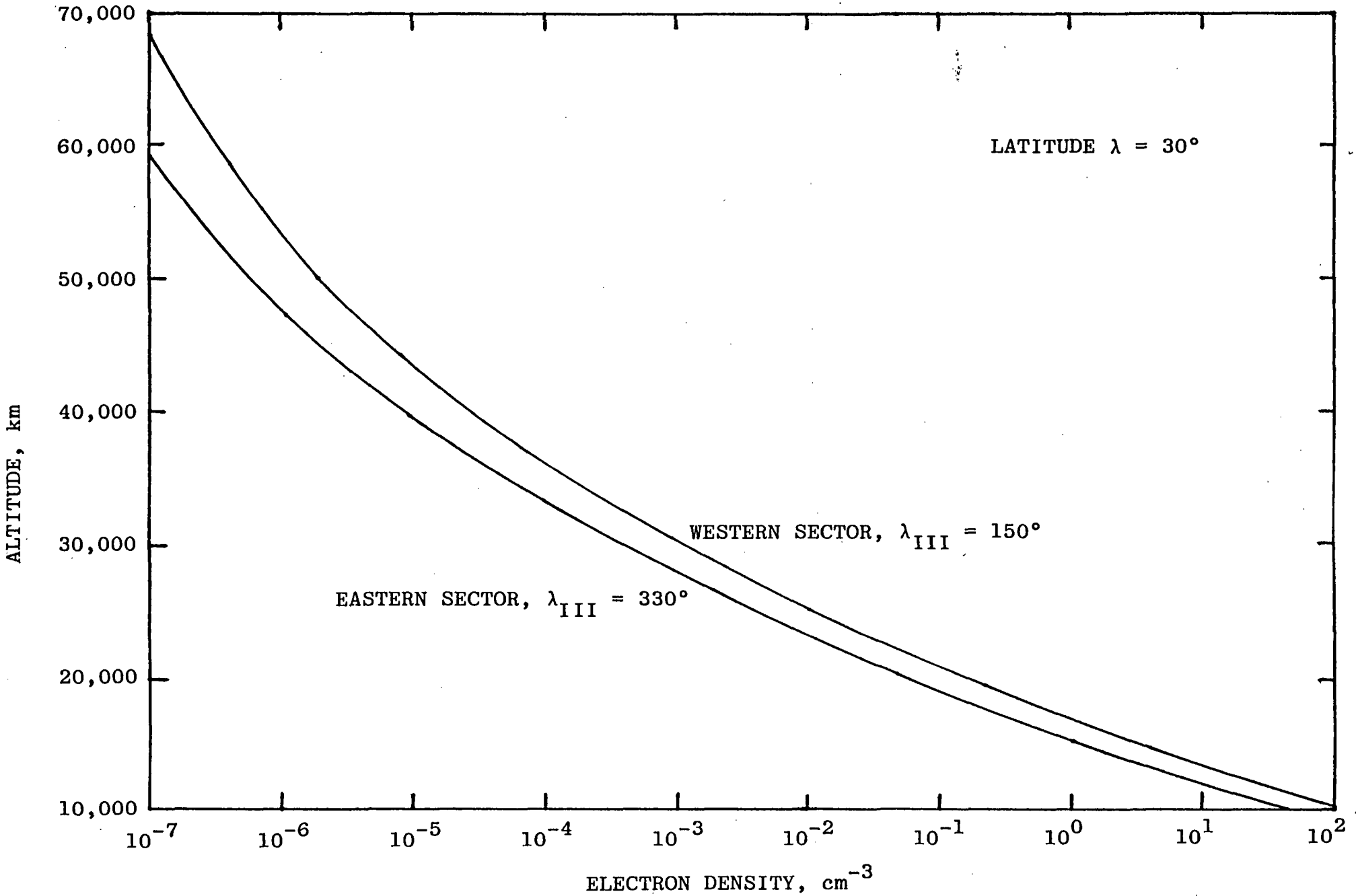

Fig.9. Vertical profiles of electron density in the plasmaspheres at latitude $\lambda = 30°$ in the Western ($\lambda_{III} = 150°$) and Eastern ($\lambda_{III} = 330°$) Sectors.

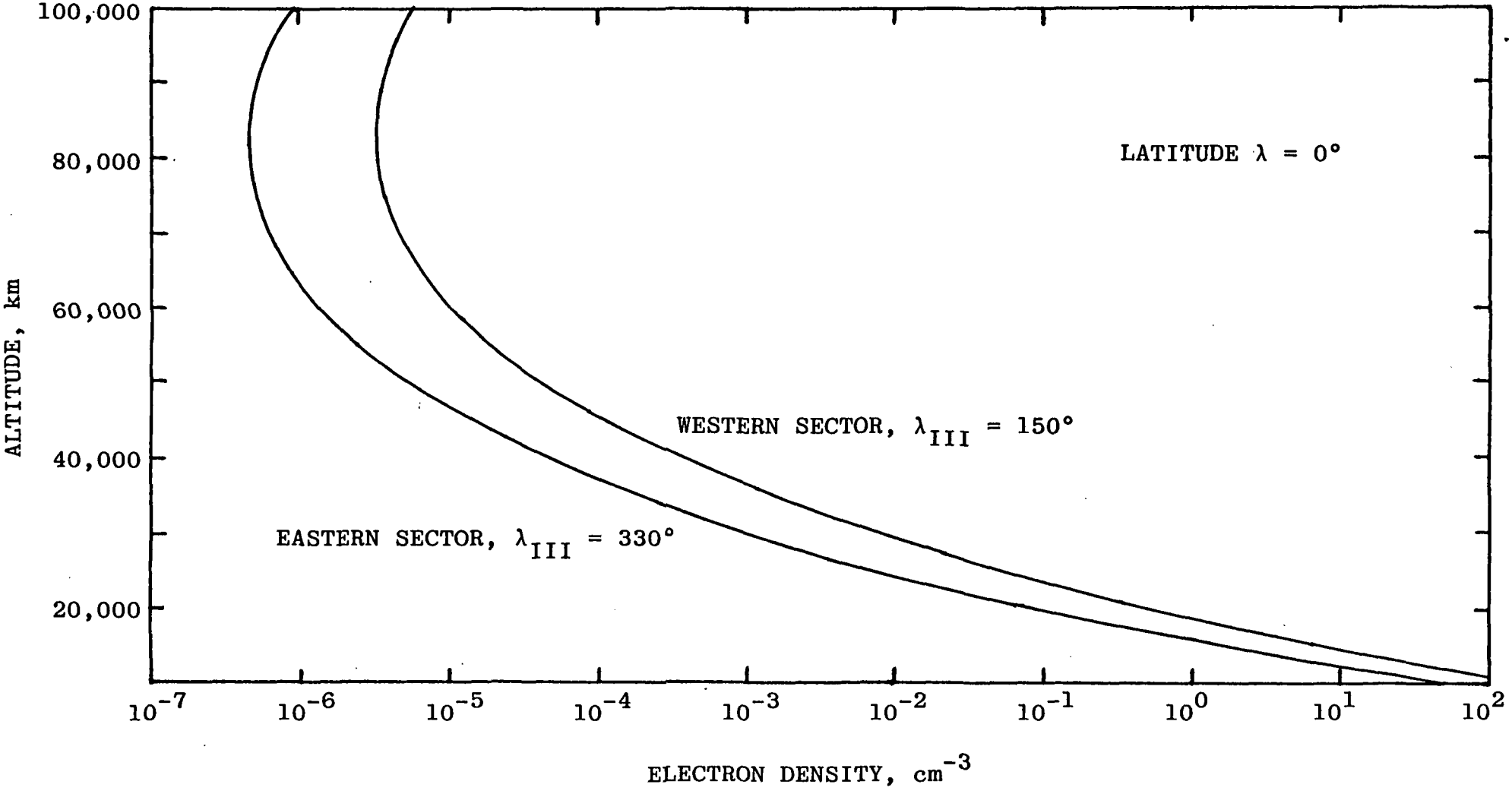

Fig.10. Vertical profiles of electron density in the equatorial plasmaspheres ($\lambda = 0°$) in the Western ($\lambda_{III} = 150°$) and Eastern ($\lambda_{III} = 330°$) Sectors showing minima in the electron density.

The Jovian Plasmasphere in Offset Dipole Model*

A Tan (Department of Physics, Alabama A&M University, Normal, AL 35762; 205-851-5313)

The magnetic field of Jupiter can be approximated by that of a dipole situated in the equatorial plane at a distance of 0.1Rj from the center at longitude 150° in System III. The offset effect would be most prominent in the meridional planes of longitudes 150° (Western Sector) and 330° (Eastern Sector). A diffusive equilibrium model in an offset dipole approximation is constructed to study the ionization patterns in the two sectors. The electron density is generally greater in the Western Sector than in the Eastern. The plasma scale height is also higher in the Western Sector. The plasma scale height is greater at the equator than at a midlatitude location (λ = 30°). Even if the peak electron density is assumed lower at the equator to reflect equatorial anomaly, at plasmaspheric heights, the electron density above the equator exceeds that at midlatitide regions, owing to the centrifugal dispersion of plasma there.

*This study was supported by NASA Grant NAGW-1067.

1.1990 Fall Meeting

2.000607177

3.(a) Box 447
Normal, AL 35762

(b) 205-851-5313

4.SA

5.(a)
(b) 5729 Ionospheres
(c)

6.

7.0%

8.$50 check enclosed

9.C

10.Request Oral Presentation
or PO (Publication only)
Do not request Poster

11.No

REVISION